Temporal Notch Disruption Uncouples Maturation from Trans-differentiation in Normal Fracture Healing

Fatma Betul Kabadas[1], Konrad Lautenschlager[1], Jacob Noorily[1], Andrew Coon[1], Madison Buckles[1], Emma Wessels[1], Christina Capobianco[1], Alexis Donneys[1], Ivo Kalajzic[2], Kurt D. Hankenson[1]

[1]Department of Orthopaedic Surgery, University of Michigan Medical School, Ann Arbor, MI 48109

[2]University of Connecticut Health Science Center, Farmington, CT 06030

fatmakab@umich.edu

Disclosures: The authors do not have anything to disclose.

INTRODUCTION: Endochondral fracture repair proceeds through a transient cartilage intermediate in which chondrocytes hypertrophy and the cartilaginous template is subsequently replaced by bone. Upon reaching hypertrophy, chondrocytes are proposed to adopt two principal fates: (i) apoptosis, generating lacunar space that permits vascular invasion and ingress of osteoprogenitors; or (ii) direct trans-differentiation to osteoblasts (OB), typically preceded by matrix and/or pericellular mineralization and activation of an osteogenic transcriptional program. Notch signaling governs skeletal lineage allocation, yet whether it licenses hypertrophic chondrocytes (HC) to exit the cartilage state and assume osteoblastic identity during repair remains unresolved. Motivated by our prior observation of cartilage persistence in a Jagged1/Jagged2 (Jag1/Jag2) Rosa-CreERT2 double-knockout (DKO) model, we designed the present study to test, with temporal precision, whether Notch signaling is required for HC-to-OB trans-differentiation during the late cartilage/early ossification phase and whether acute Notch perturbation concomitantly alters angiogenesis at the cartilage-bone interface (transition zone, TZ).

METHODS: Adult C57Bl/6 mice (14–18 weeks; mean ≈ 16 weeks n=5M, 3F) underwent standardized mid-diaphyseal transverse tibial fracture with intramedullary fixation under IACUC approval. In the primary pharmacologic cohort, canonical Notch signaling was inhibited with dibenzazepine (DBZ, Tocris, 10 µmol/kg i.p.) formulated in soluble methylcellulose, given once daily 10–14 days post-fracture (dpf). Vehicle mice received methylcellulose on the same schedule, and calluses were harvested 15 dpf. An independent Jag1/Jag2 Rosa-Cre-DKO cohort was analyzed at day 15 with Jag1/Jag2 deletion present from 0–15 dpf. Due to the timing and mechanism of Notch inhibition (late pharmacologic vs early, broad genetic), models were analyzed separately and not pooled. Paraffin sections (5µm) were stained with Safranin O/Fast Green for prespecified morphometrics. For both cohorts, type X collagen area was quantified by immunofluorescence (IF) co-stained with endomucin (Emcn) using preset acquisition settings held constant within experiments. In DBZ, type X collagen immunohistochemistry (DAB staining) images are qualitative, quantitative inferences relied on immunofluorescence. The TZ was defined by tracing the cartilage-bone interface and dilating outward to a fixed 1000 µm band; DAPI and Emcn masks were generated under uniform processing, and Emcn+ cells were defined by ≥ 50% overlap of each DAPI nucleus with the Emcn mask. Bulk callus RNA was profiled by SYBR qPCR (ΔCt) for Notch targets (*Hey2/L*), chondrogenic (*Sox9, Col10a*), and osteogenic (*Runx2, Sp7/Osterix, Bglap/Osteocalcin, Col1a1*) markers with the same pipeline applied to DKO. Two-sided unpaired t-tests compared DBZ vs vehicle and DKO vs wild type (WT) within model ($\alpha = 0.05$).

RESULTS SECTION: DBZ administered on 10-14 dpf reduced expression of the canonical Notch target *Hey2* **(Fig. 1A)**, consistent with on-target γ-secretase activity and corroborated by gastrointestinal toxicity observed in DBZ-treated mice **(data not shown)**. Cartilage morphometry indicated preserved early chondrogenesis but a relative accumulation of mature hypertrophic chondrocytes, reflected by a higher (ns) mature-hypertrophic cartilage area (MHCA)/hypertrophic cartilage area (HCA) ratio **(Fig. 1B)**. Consistent with this, type X collagen IF normalized to cartilage area was higher (ns) in DBZ-treated fractures **(Fig. 1B).** This was further corroborated by the attenuation of the osteogenic gene markers: *Osteocalcin* decreased by ~74% (p= 0.049), while *Runx2*, *BSP*, *Col1a1*, and *Osterix* were lower (ns); *Sox9* were higher (ns) **(Fig. 1A)**. Within the fixed 1000-µm TZ, Emcn+ endothelial density was higher (ns), and TZ/HCA was lower (−39%, p = 0.1638) **(Fig. 1C).** In contrast, in the Jag1/Jag2 Rosa-Cre model, morphometry supported a cartilage maturation delay rather than a trans-differentiation defect. IHCA/MHCA was significantly higher in Cre+ calluses (+427%, p=0.0131) **(Fig. 1D)**. Emcn+/DAPI+ within the TZ was comparable to WT, whereas TZ/HCA was lower (ns), again consistent with a delayed positional advance **(Fig. 1C)**. Bulk RNA qPCR of the Rosa model showed lower Notch targets (p=0.0023) but unchanged osteogenic and chondrogenic transcripts at day 15 **(Fig. 1A)**. Taken together, the results of the genetic model indicate a defect in pre-hypertrophic maturation, whereas later-stage γ-secretase inhibition is most consistent with impaired hypertrophic chondrocyte-to-osteoblast trans-differentiation.

DISCUSSION: The two perturbation models point to stage-specific requirements for Jagged-Notch signaling in endochondral repair. When Jag1/Jag2 are deleted starting 0 dpf in the Rosa-Cre-DKO mice, the callus has a larger cartilage burden and morphometry favors the accumulation of immature over mature hypertrophic cartilage (significantly higher IHCA/MHCA), consistent with a hypertrophic maturation delay rather than a failure of the terminal steps in endochondral ossification. By contrast, late γ-secretase inhibition (DBZ, 10-14 dpf) preserved early chondrogenesis but shifted the composition within the hypertrophic compartment toward mature hypertrophic chondrocytes (higher MHCA/HCA with lower IHCA/HCA) and reduced osteogenic transcripts—most notably *Osteocalcin*—supporting a defect in hypertrophic chondrocyte-to-osteoblast trans-differentiation at this later stage. Changes in the TZ align with this interpretation. In both models the TZ/HCA ratio was lower, indicating a delayed advance of the cartilage-bone interface. In the DBZ cohort, Emcn-labeled endothelial density/area within the fixed TZ band was numerically higher, consistent with persistent cartilage and hypoxia generating pro-angiogenic signals (e.g., VEGF) despite delayed ossification. In the Rosa model, Emcn+/DAPI+ was not increased, which is plausible given that Jag1/Jag2 loss spans multiple compartments (chondrocytes, endothelium, immune cells) from the outset and may blunt vascular expansion, whereas in the DBZ design the vascular network is largely established before inhibition begins at 10 dpf. Several caveats temper these conclusions. The DBZ cohort and TZ analyses were underpowered, and bulk RNA analysis dilutes cell-type specific changes. Non-significant directional differences are reported for completeness and interpreted cautiously. Future work should increase sample size, incorporate lineage tracing to verify the fate of hypertrophic chondrocytes, apply single-cell or spatial transcriptomics to resolve cell-type–specific Notch responses, quantify apoptosis and mineralization directly, and dissect endothelial versus chondrocyte autonomy with compartment-specific Notch manipulations. Together, the data support a model in which early Jagged-Notch signaling licenses hypertrophic maturation, whereas Notch signaling during late endochondral ossification promotes hypertrophic chondrocytes to transdifferentiate into osteoblasts, with vascular changes reflecting the altered tempo of cartilage resolution rather than being the primary rate-limiting step.

SIGNIFICANCE/CLINICAL RELEVANCE: Our findings hint that the timing of Notch/Jagged activity may influence the cartilage-to-bone transition; if borne out in larger studies, timing-aware pathway modulation could be considered in the design of improved osteogenic therapeutics intended for clinical use.

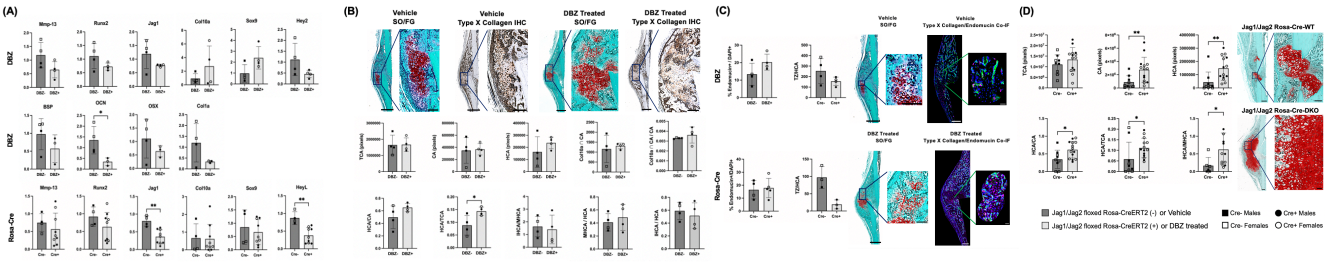

Figure 1. Notch–Jagged perturbation reveals stage-specific failures in endochondral repair: early Jag1/Jag2 loss delays pre-hypertrophic maturation and slows overall callus transition, whereas late γ-secretase blockade slows HC-to-osteoblast trans-differentiation, leading to accumulation of mature HCs and increased transition-zone angiogenesis. (A) Bulk RNA qPCR (both models). qPCR for Notch targets (*Hey2/HeyL*), chondrogenic (*Sox9*), and osteogenic (*Runx2, Sp7/Osterix, Bglap/Osteocalcin, Col1a1*); data as $\log_2$ fold change relative to controls. n = vehicle 4, DBZ 4; WT 4, DKO 7. **(B) Pharmacologic Notch inhibition (vehicle vs dibenzazepine) - morphometrics and type X collagen.** 4x SO/FG overviews/zooms plus adjacent-section type X collagen IHC; graphs show morphometrics and type X collagen quantification based on IF. n = vehicle 4, DBZ 4. **(C) Transition zone and vascular labeling (both models).** 4x SO/FG images with TZ defined as a fixed 1,000 µm band; 10x Endomucin + type X collagen IF images. Graphs show %Endomucin+/DAPI+ within TZ (Endomucin+ nucleus = ≥50% overlap with Endomucin mask) and TZ/CA. n = vehicle 4, DBZ 4; WT 3, DKO 3. **(D) Jag1/Jag2 Rosa-Cre-DKO or WT - cartilage morphometrics.** 10x SO/FG overviews with boxed ROIs and matched zooms; graphs show prespecified morphometric endpoints. n = WT 9, DKO 14. Common details: Points = individual calluses; bars = mean ± SEM; two-sided unpaired t-tests. Scale bars: 500 µm (overviews) and 100 µm (zooms). Acquisition settings were held constant within each panel. **Abbreviations (Panels B & D):** TCA, total callus area; CA, cartilage area; HCA, hypertrophic cartilage area; MHCA, mature hypertrophic cartilage area; IHCA, immature (pre-hypertrophic) cartilage area.